JOURNAL OF CATALYSIS 152, 331–340 (1995)

Influence of Carrier Doping on the Interaction of Benzene and Toluene with Supported Rhodium

T. Ioannides, M. Tsapatsis, M. Koussathana, and X. E. Verykios

Institute of Chemical Engineering and High Temperature Chemical Processes, Department of Chemical Engineering, University of Patras, GR 265 00, Patras, Greece

Received June 15, 1994; revised October 10, 1994

The interaction of benzene and toluene with rhodium crystallites dispersed on TiO_2 carriers doped with W^{6+} cations of variable concentration is investigated employing steady-state hydrogenation, competitive hydrogenation, temperature-programmed desorption (TPD) and temperature-programmed surface reaction (TPSR). Turnover frequencies of both hydrogenation reactions are enhanced when Rh is dispersed on W^{6+}-doped TiO_2, while the ratio of the adsorption coefficients of toluene to benzene is reduced. The latter result implies that the toluene–Rh interaction has been weakened to a larger extent than the benzene–Rh interaction. TPD and TPSR experiments also reveal weakened adsorption bonds of benzene and toluene with Rh supported on doped TiO_2. These observations are discussed with respect to short-range and long-range electronic interactions at the metal–support interface, evoking the theory of metal–semiconductor contacts. © 1995 Academic Press, Inc.

INTRODUCTION

Various forms of interaction between metal crystallites and support materials in supported metal catalysts have been cited in the literature. The concept of Strong Metal–Support Interactions (SMSI), which dominated the literature of the previous decade, is a classical example of this issue. The origin or the mechanism of these interactions has often been the subject of controversy. In most cases, the influence of the carrier on kinetic and chemisorptive parameters of the metal crystallites has been interpreted either by a geometric reasoning (1–3) or by an electronic one (4). The two theories have often been merged so as to explain experimental observations (5).

The effects of altervalent cation doping of the support on the catalytic behavior of the supported metal have been initially studied by Schwab (6) and Solymosi (7). The effects of altervalent cation doping of TiO_2 carriers on chemisorptive and catalytic properties of Group VIII metal crystallites were investigated by Verykios and coworkers (8–15) and the results were interpreted in terms of electronic interactions at the metal–semiconductor interface. As a result of these interactions, the work function of surface metal atoms may be altered, which results in significant alterations of chemisorptive and kinetic parameters. Similar electronic-type interpretations have been proposed by other investigators of similar or other systems (16, 17).

The effect of alterations of the metal work function on catalyst behavior has been studied by Vayenas *et al.* (18, and references therein) in the framework of the phenomenon of Nonfaradaic Electrochemical Modification of Catalytic Activity (NEMCA). The phenomenon refers to reversible catalytic activity and selectivity modifications of metal catalysts by electrochemically supplying oxygen anions onto metal surfaces via polarized solid electrolyte cells.

The influence of altervalent cation doping of TiO_2 supports on the chemisorptive and catalytic properties of Rh crystallites, reduced at low temperatures (200–250°C) to avoid the onset of the SMSI phenomenon, was discussed in previous publications (13, 15). It was shown that the H_2 and CO adsorption capacity of Rh is significantly altered upon doping the carrier (TiO_2) with altervalent cations, while the Rh–CO bond is weakened. Alterations in turnover frequencies of CO and CO_2 hydrogenation and CO oxidation as well as in activation energies of the same reactions were also observed. The magnitude of these alterations was found to be a function of the concentration of the doping cation (W^{6+}) in the crystal matrix of the carrier. It has also been shown that the observed experimental findings are not related to the SMSI phenomenon (15).

The present communication supplies additional evidence of electronic modification of metal surfaces by altervalent cation doping of the carrier, via the competitive benzene–toluene hydrogenation reactions. This reaction system has been employed to monitor alterations of the electronic structure of metal surfaces by many investigators (19–22) and it is based on the fact that toluene is more of an electron-donor than benzene and, thus, the relative rates of hydrogenation of the two molecules depend strongly on the electronic configuration of the sur-

0021-9517/95 $6.00

face. On the other hand, the rates of hydrogenation are not sensitive to the details of the geometric structure of the surfaces; thus the two factors can be decoupled. This concept has been used by Frank and Gil (19) to study the nickel promoting effect of tungsten sulfide catalysts and the influence of sulfur on the catalytic properties of Pt. Similarly, Tri *et al.* (20) used the same system to monitor electronic changes of Pt in Pt–Mo and Pt–Ce catalysts and to determine intrinsic changes in the electronic structure of different Group VIII metals.

EXPERIMENTAL

(*a*) *Catalyst Preparation and Characterization*

Preparation and characterization of doped supports has been described in detail in previous publications (8, 10, 13). As in previous cases, the parent TiO_2 support was obtained from Degussa (P-25) and it was doped with W^{6+} cations using WO_3 as the precursor compound, employing the method of high-temperature diffusion. Catalysts were prepared by incipient wetness impregnation of the support with appropriate amounts of aqueous solutions of $RhCl_3$. Impregnated supports were dried for 24 h at 110°C and reduced in flowing hydrogen at 200 and 250°C for a total period of 2 h. Metal content of all catalysts was invariably 0.5 wt%. Further details have been reported previously (13), along with catalyst characterization procedures.

(*b*) *Determination of Reaction Rates*

Benzene and toluene hydrogenation and benzene/toluene competitive hydrogenation were performed in a conventional flow microreactor operating at atmospheric pressure, at 30°C. Hydrogen and benzene or toluene partial pressures were kept constant at 83 kPa and 1.6 kPa, respectively. Nitrogen gas was used as a diluent. Benzene and toluene partial pressures were established by hydrogen flow through two saturators containing the hydrocarbons, immersed in constant temperature baths. The feed mixture was periodically analyzed before entering the reactor.

Before initiation of any reactions, the catalyst was exposed to hydrogen flow at 200°C for 2 h. A similar pretreatment for 30 min was also conducted between runs on the same catalyst. Analysis of the product mixture was performed on a gas chromatograph (Hewlett-Packard, model 5890) equipped with a flame ionization detector, an automatic gas sampling valve and an electronic integrator. A packed Carbowax-20M column separated benzene, toluene, cyclohexane, and methylcyclohexane. In all cases, conversion was maintained below 10%.

(*c*) *Temperature-Programmed Desorption (TPD) and Temperature-Programmed Surface Reaction (TPSR)*

The TPD apparatus has been described in detail in a previous publication (23). Prior to any experiments it was determined that the TPD cell or the tubing were not active in the adsorption of benzene or toluene and did not contribute to the mass spectrometer signal. The procedure for each experiment was the following. The catalyst was placed in the TPD cell, supported by quartz wool, and heated to 250°C in H_2 flow for 1 h. It was then cooled under He flow. When the desired adsorption temperature was reached, the He flow was switched to benzene/N_2 or toluene/N_2 flow. Benzene and toluene concentrations in these streams were approximately 10 and 3 mol%, respectively. After 15 min, the flow was switched to He and the lines were cleaned for 3 min. Temperature programming was then initiated and the TPD profiles were obtained. At the end of each experiment, the catalyst was exposed to O_2 at 450°C for 5 min to burn off carbon deposits. This procedure was found to give reproducible TPD and TPSR results.

RESULTS

The influence of altervalent cation doping of the carrier (TiO_2) on chemisorptive and kinetic parameters of supported Rh catalysts was discussed in previous publications (13–15). It was found that the chemisorptive capacity of doped catalysts for hydrogen, as well as the activity of Rh in the CO and CO_2 hydrogenation reactions, are significantly enhanced. The properties of $Rh/TiO_2(W^{6+})$ catalysts are further investigated in the present communication employing benzene and toluene as probe molecules and their competitive hydrogenation as probe reaction.

(*a*) *Influence of Carrier Doping on Kinetic Parameters*

The influence of doping of the TiO_2 carrier with W^{6+} cations, at concentrations in the range of 0–0.45 at.%, on the specific activity of Rh for benzene and toluene hydrogenation is illustrated in Fig. 1. The kinetic experiments pertaining to the results shown in Fig. 1 were carried out at a temperature of 30°C and atmospheric pressure, with a hydrogen-to-hydrocarbon partial pressure ratio of 50. There is always difficulty in expressing turnover frequencies when employing catalysts which exhibit abnormal chemisorption capacity, since chemisorption techniques are often used to estimate the degree of dispersion. As shown previously (13), these 0.5% $Rh/TiO_2(W^{6+})$ catalysts exhibit abnormally high H_2 adsorption capacity, which increases with increasing dopant concentration. It was also shown, however, that altervalent cation doping of the carrier does not influence, to a great extent, the degree of dispersion of the metal. Thus, in the present

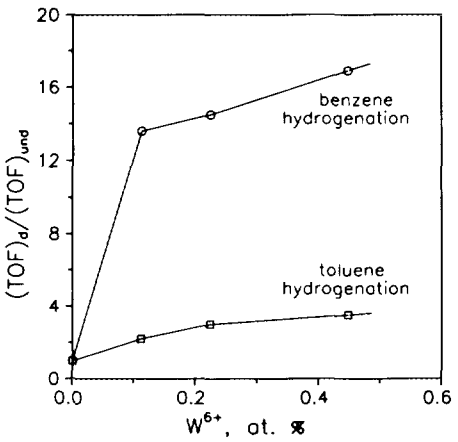

FIG. 1. Influence of the concentration of the dopant (W^{6+}) in the carrier (TiO_2) matrix on specific activity of Rh for benzene and toluene hydrogenation.

study, as in previous ones, turnover frequencies of benzene and toluene hydrogenation are estimated on the basis of the dispersion observed over the undoped catalyst.

The ratio of turnover frequencies observed with the doped catalysts over that observed with the undoped catalyst is shown in Fig. 1 as a function of the dopant concentration in the TiO_2 carrier, in atom %. It is apparent that Rh dispersed on W^{6+}-doped TiO_2 carriers exhibits enhanced activity for both benzene and toluene hydrogenation. The degree of enhancement is significantly higher in the case of benzene hydrogenation and it is more pronounced at the 0.11 at.% W^{6+}-dopant level, leveling-off at higher dopant concentrations.

The influence of higher-valence cation doping of TiO_2 carriers on the catalytic performance of Rh surfaces was also investigated under competitive benzene/toluene hydrogenation conditions. Under the assumption of competitive adsorption of benzene and toluene on a metallic surface and constant hydrogen partial pressure, a Langmuir–Hinshelwood rate expression for benzene hydrogenation in the presence of toluene assumes the form

$$r_B^{(T)} = \frac{k_B K_B P_B}{1 + K_B P_B + K_T P_T} \qquad [1]$$

where k and K are reaction rate and adsorption equilibrium constants, respectively. If, furthermore, it is assumed that $1 \ll K_B P_B$ and $1 \ll K_T P_T$, then the ratio of the rate of benzene hydrogenation in the absence of toluene (r_B^0) over that in the presence of toluene ($r_B^{(T)}$) reduces to the form:

$$\frac{r_B^0}{r_B^{(T)}} = 1 + \frac{K_T}{K_B}\frac{P_T}{P_B} \qquad [2]$$

Further details of this derivation can be found elsewhere (20–22).

The ratio of the adsorption equilibrium constants, $K_T/K_B = K_{T/B}$, can be obtained from Eq. 2 from results of experiments in which the relative partial pressures of benzene and toluene are varied, while the partial pressure of hydrogen is maintained constant. In the present study, the partial pressure of benzene was also maintained constant at 1.6 kPa, while the partial pressure of toluene was varied in the range of 0–1 kPa.

The parameter $K_{T/B}$ defines, to a large extent, the relative strength of the adsorption bonds of benzene and toluene on metallic surfaces. Large values of this parameter imply that the surface has a much higher affinity for toluene than for benzene. Because of the effect of the methyl group, toluene is a better electron donor than benzene and is expected to adsorb more strongly on metal surfaces. There is theoretical (24) as well as experimental (25) evidence in support of this view. This is reflected in $K_{T/B}$ values larger than unity. These considerations are of course valid only as long as benzene and toluene are competitively adsorbed and with the same mode on the surface, and nondissociatively.

The application of Eq. [2] in the analysis of data obtained in the present study is shown in Fig. 2, in which relative rates of benzene hydrogenation in the absence and presence of toluene ($r_B^0/r_B^{(T)}$) are shown as a function of the relative pressures of toluene to benzene (p_T/p_B) for Rh catalysts dispersed on TiO_2 doped with W^{6+} cations of variable concentration. It is observed that the linearity of Eq. [2] is satisfied to a good extent. The slopes of the resulting lines are equal to $K_{T/B}$. It is apparent that the $K_{T/B}$ values, or relative strengths of toluene and benzene

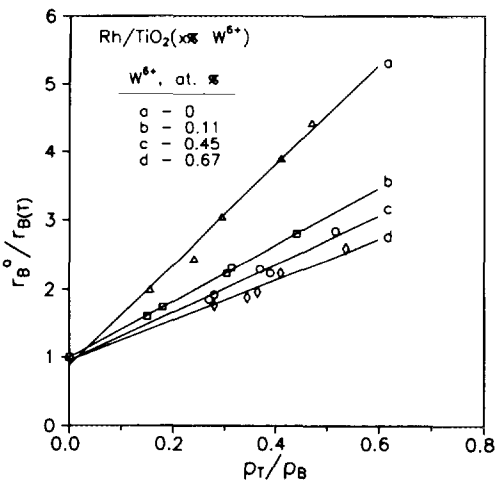

FIG. 2. Determination of the ratio of adsorption equilibrium constants of toluene to benzene, under conditions of competitive benzene/toluene hydrogenation over $Rh/TiO_2(x\%\ W^{6+})$ catalysts.

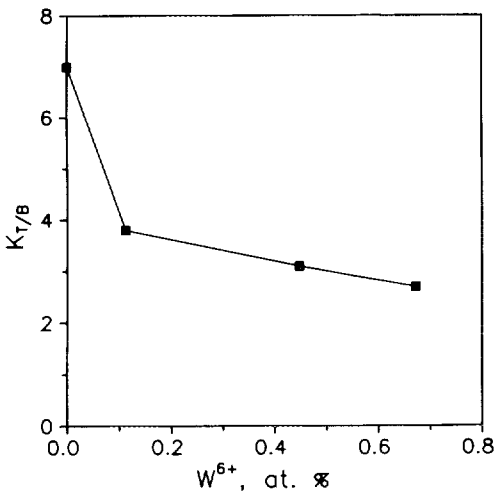

FIG. 3. Variation of the ratio of adsorption equilibrium constants of toluene to benzene with dopant concentration in the carrier of 0.5% $Rh/TiO_2(x\%\ W^{6+})$ catalysts.

adsorption on Rh, are a function of the concentration of the dopant in the carrier. This is illustrated in Fig. 3 in which $K_{T/B}$ values of Rh catalysts are shown as a function of the dopant content of the carrier. In all cases, $K_{T/B}$ values are larger than unity, since toluene is more strongly adsorbed on metallic surfaces than benzene. However, $K_{T/B}$ values decrease significantly upon doping of the carrier with W^{6+} cations and they exhibit a monotonic reduction with increasing dopant concentration.

(*b*) *Temperature-Programmed Desorption and Temperature-Programmed Surface Reaction Studies*

The desorption characteristics of benzene and toluene adsorbed on Rh crystallites dispersed on W^{6+}-doped TiO_2 carriers were investigated by TPD and TPSR techniques. Four kinds of experiments were performed: (a) TPD from unmetallized carriers following room-temperature adsorption, (b) TPD from Rh/TiO_2 (W^{6+}) catalysts, following room-temperature adsorption, (c) TPD following room-temperature adsorption and exposure to H_2 flow at 25, 65, and 115°C, (d) TPSR under H_2 flow following benzene or toluene adsorption.

(b-1) TPD from unmetallized carriers. It is well-known that benzene and toluene adsorb on TiO_2 (26–28), as well as on other metal oxide surfaces (26, 29, 30). Thus, it is essential to conduct TPD experiments from carriers in the absence of Rh, in order to be able to distinguish species originating from the metal from those originating from the carrier. All carriers employed in the present study were exposed to a stream containing benzene (10 kPa) or toluene (3 kPa) in N_2 for 15 min. The flow was subsequently switched to He for 3 min to remove gas phase hydrocarbons and temperature programming was initiated. In all cases, the resulting TPD profiles consisted of a single symmetric peak, corresponding to either benzene or toluene. Peak maxima, reported in Table 1, indicate that toluene desorbs at temperatures higher than those of benzene, as expected from the difference in the boiling point of the two molecules. This, however, may also imply that the adsorption bond of toluene with the metal oxide surface is stronger, in agreement with results obtained by Suda (27) and Nagao and Suda (28). A shift towards higher desorption temperatures is also observed with increasing W^{6+}-dopant concentration in the carrier, but this can be attributed in part to readsorption effects. The reactivity of benzene and toluene adsorbed on the surface of the carriers was also investigated by exposing them to H_2 flow at room temperature. No hydrogenation products were detected, indicating that the carriers, in the absence of metal, do not adsorb hydrogen dissociatively, so as to proceed to the hydrogenation of the aromatic molecules.

(b-2) TPD from $Rh/TiO_2(W^{6+})$ catalysts. TPD profiles obtained following benzene adsorption on Rh/TiO_2 ($x\%W^{6+}$) catalysts are shown in Fig. 4. Only benzene and hydrogen were detected in the gas phase during the TPD experiments. This is in agreement with results obtained during TPD from Rh(111) under UHV conditions (31). The low-temperature benzene peak (Fig. 4a) was also observed in the case of TPD from the bare supports. Thus, this peak is attributed to benzene adsorbed on the carrier. A small contribution to this peak from benzene physisorbed on the Rh surface cannot, however, be excluded. The quantity of benzene desorbing molecularly from Rh surfaces (high-temperature peak in Fig. 4a) is observed to increase with increasing W^{6+}-dopant concentration in the carrier. The peak temperature is in the neighborhood of 250°C, with a small shift to 240°C over the Rh/TiO_2 (0.67% W^{6+}) sample. The hydrogen profiles (Fig. 4b) are similar in all cases, with a single desorption peak at 250–255°C, with the exception of Rh/TiO_2(0.45% W^{6+}) in

TABLE 1

Peak Maxima (T_m) of Benzene and Toluene Desorption from $TiO_2(x\%\ W^{6+})$ Carriers

Carrier	T_m, (°C)	
	Benzene	Toluene
TiO_2	62	72
TiO_2 (0.11% W^{6+})	66	83
TiO_2 (0.22% W^{6+})	72	89
TiO_2 (0.45% W^{6+})	82	96
TiO_2 (0.67% W^{6+})	88	105

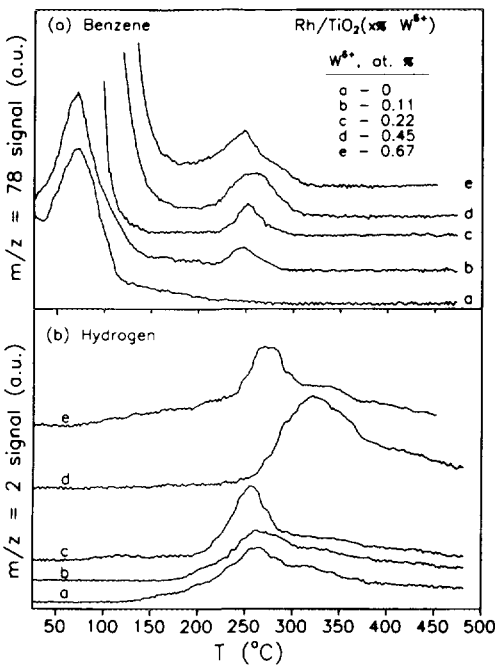

FIG. 4. TPD profiles of benzene (a) and hydrogen (b) following benzene adsorption at 25°C on 0.5% $Rh/TiO_2(x\%\ W^{6+})$ catalysts.

which the H_2 peak is shifted to 310–320°C. The H_2 peak appears at approximately the same temperature as that of benzene indicating that desorption and dehydrogenation processes occur competitively during the TPD experiment.

The quantity of adsorbed benzene which is dehydrogenated and detected as H_2 and the quantity which desorbs molecularly were estimated from the profiles of Fig. 4. The quantity of benzene that desorbs molecularly is small, corresponding to ~5% of the total quantity of adsorbed benzene. Based on the results of Koel *et al.* (31), it can be assumed that at the end of the TPD experiment benzene is fully dehydrogenated and only carbon remains on the Rh surface. The benzene surface coverage can then be estimated for the $Rh/TiO_2(0\%\ W^{6+})$ catalyst, whose dispersion is well known (0.10), and it was found to be 0.45. This value is in good agreement with benzene surface coverage values for Rh/Al_2O_3 and Rh/SiO_2 catalysts, which have been reported previously (26). The benzene surface coverage on Rh(111), at saturation conditions, has been reported to be in the neighborhood of 0.13–0.17 (31, 32). Therefore, it seems that small Rh crystallites dispersed on carriers can adsorb 2–3 times more benzene than the (111) crystallographic plane. This has also been observed on other metals, such as Pt/Al_2O_3, where benzene surface coverage has been reported to be 0.31 (33) and for Ni, where the corresponding parameter can be estimated to 0.43 (34, 35). This observation can be explained assuming that the C–H bonds can form an angle with the surface upon adsorption (32, 36) leading to enhanced surface coverage, or that a fraction of adsorbed benzene is bound to the surface by σ-bonds (37–39) or that new adsorption sites are created at the metal–support interfacial area, in which the benzene molecule is bound to both the metal and the carrier.

The TPD profiles shown in Fig. 4 also reveal a significant increase in the amount of molecularly desorbing benzene with increasing dopant concentration in the carrier. This is an important observation taking into consideration that no molecularly desorbing benzene is detected from the undoped catalyst or from Rh/SiO_2 catalysts (26), and that one of the most significant differences of Group VIII metals concerning the characteristics of benzene adsorption is the fraction of molecularly desorbing benzene. For Pt(111) the fraction of benzene that desorbs molecularly is about 50% at monolayer coverage (25). For Rh(111) it is about 15% (31) and for Ru(001) only 5% (40). A strong *M*–C bond leads to weak C–H bonds in adsorbed benzene, which then has a larger tendency towards dehydrogenation (40). In this sense, it can be said that benzene adsorbs more strongly on Ru than on Pt. The fraction of molecularly desorbing benzene is, therefore, a good indicator of the relative strength of the adsorption bonds, a parameter which cannot be easily detected from the TPD profiles, because of the competitive nature of the dehydrogenation and desorption processes. It can thus be inferred that the Rh-benzene adsorption bonds are weakened as a result of higher-valence doping of the TiO_2 carriers.

TPD profiles obtained following toluene adsorption on $Rh/TiO_2(x\%\ W^{6+})$ catalysts are shown in Fig. 5. The profiles of molecularly desorbed toluene (not shown) were found to be similar to those obtained over the unmetallized

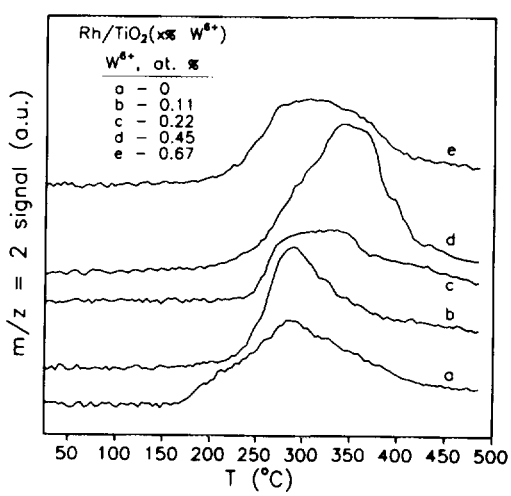

FIG. 5. TPD profiles of hydrogen following toluene adsorption at 25°C on 0.5% $Rh/TiO_2(x\%\ W^{6+})$ catalysts.

carriers, indicating that no molecular toluene desorbs from Rh surfaces. Based on the discussion of the previous paragraph, this is an indication that toluene is more strongly adsorbed on Rh than benzene. Similar observations have been made with Pt (25). Therefore, only the H_2 profiles are shown in Fig. 5. The H_2 profiles consist of broad peaks exhibiting maxima in the temperature range of 270–300°C, with the exception of the Rh/TiO_2(0.45% W^{6+}) catalyst, whose peak temperature is somewhat higher (~350°C). This catalyst exhibited a similar behavior under benzene TPD. Since no other desorption products were detected, the quantity of desorbed H_2 was used to estimate the quantity of adsorbed toluene, assuming that toluene fully decomposes according to: $C_7H_8(ads) \rightarrow 4H_2 + 7C(ads)$ and that at the end of the TPD experiment only carbon remains on the surface. The quantity of adsorbed toluene was found to be comparable, although somewhat smaller, than the quantity of adsorbed benzene. The toluene surface coverage of the undoped catalyst was estimated to be approximately 0.35, compared to 0.45 for benzene, indicating that the modes of adsorption of the two molecules on the Rh surface are similar. The TPD profiles of Fig. 5 also indicate that the temperature of initiation of the decomposition reaction (H_2 detection) increases with increasing dopant concentration, indicating that the tendency of adsorbed toluene to decompose decreases with increasing W^{6+}-dopant concentration in the TiO_2 matrix.

(b-3) Reactivity of adsorbed benzene and toluene. The hydrogenation reactivity of adsorbed benzene and toluene was investigated with the following methodology. After benzene or toluene adsorption at room temperature, the gas flow was switched from He to H_2 at temperatures of 25, 65, and 115°C, and maintained for 5 min prior to obtaining TPD profiles. These profiles indicate the quantities of benzene or toluene remaining unreacted on the Rh surface after this treatment. TPD profiles obtained over the undoped catalyst and the 0.67% W^{6+}-doped catalyst are shown in Figs. 6 and 7, respectively. These profiles correspond to benzene adsorption. In all cases, benzene weakly adsorbed on the carrier surface is totally reacted (hydrogenated to cyclohexane) upon exposure of the catalysts to H_2 at 25°C. However, as indicated by the H_2 profiles (high temperature peaks), benzene strongly adsorbed on the Rh surface is weakly affected by exposure to H_2 at 25°C. At higher hydrogenation temperatures (65 and 115°C), the quantity of benzene unreacted and decomposing (as indicated by the H_2 peak) is reduced. The H_2 TPD profiles after hydrogenation of preadsorbed benzene (Figs. 6, 7) show the presence of a low-temperature hydrogen peak at about 80–100°C. This peak corresponds to desorption of molecular hydrogen and can be attributed to hydrogen adsorbed on the Rh surface during the hydrogenation step. This peak is similar to the one observed during TPD after hydrogen adsorption (13). This implies that weakly bound hydrogen (T_{des} ~ 80–100°C) is present on the Rh surface during hydrogenation and might well be the catalytically active species.

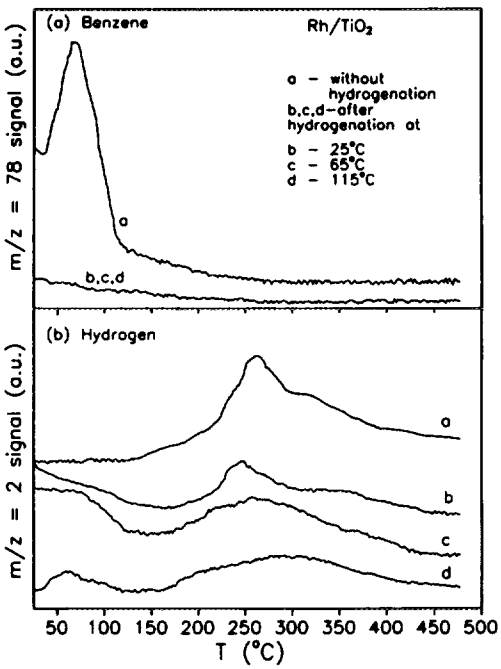

FIG. 6. TPD profiles of benzene (a) and hydrogen (b) from the undoped 0.5% Rh/TiO_2 catalyst after: (a) benzene adsorption at 25°C, and after exposure to H_2 for 5 min at (b) 25°C, (c) 65°C, (d) 115°C.

The decrease of the quantity of unreacted benzene is larger over the doped catalyst, indicating higher hydrogenation reactivity of this sample. The quantity of benzene remaining adsorbed after hydrogenation at 25, 65, and 115°C and the quantity of benzene desorbed without any prior hydrogenation treatment, are shown in Table 2. Doped catalysts seem to adsorb larger (by 20–100%) quantities of benzene. If it is assumed that the mode of benzene adsorption is the same on doped and undoped catalysts, these data can be used for the estimation of Rh dispersion on doped catalysts. It turns out that Rh dispersion is in the range of 0.12–0.20 on doped catalysts. From TEM measurements it was found that the dispersion of the Rh/TiO_2(0.22% W^{6+}) catalyst is 0.17 (13). From results in the CO oxidation reaction it was also inferred that the dispersion of doped catalysts is in the range of 0.15–0.19 (14). The very good agreement between these independent measurements must be noted. It seems, then, that the dispersion of the doped catalysts is similar, although somewhat higher than the dispersion of the undoped catalyst. In Table 2 also the ratio of the quantity of benzene remaining adsorbed after hydrogenation at 115°C over the total quantity of benzene adsorbed, as estimated from the

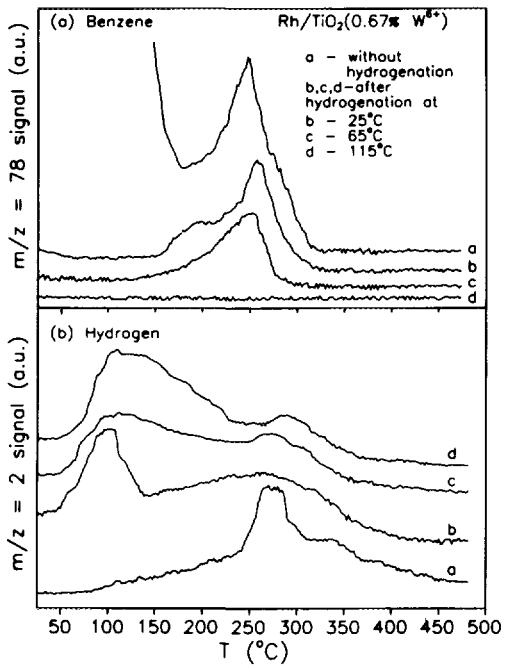

FIG. 7. TPD profiles of benzene (a) and hydrogen (b) from the 0.5% Rh/TiO_2 (0.67% W^{6+}) catalyst after: (a) benzene adsorption at 25°C, and after exposure to H_2 for 5 min at (b) 25°C, (c) 65°C, (d) 115°C.

TPD experiments without the prior hydrogenation step, R_B, is reported. This parameter expresses the reactivity of benzene adsorbed on Rh surfaces towards hydrogenation, as it tends to zero when benzene is fully reactive and to unity when it is totally unreactive. It is apparent from Table 2 that the reactivity of benzene adsorbed on Rh particles dispersed on W^{6+}-doped TiO_2 carriers towards hydrogenation is significantly higher than that observed when Rh is dispersed on undoped TiO_2.

Similar results were also obtained when toluene was adsorbed on $Rh/TiO_2(x\%W^{6+})$ catalysts and subsequently

TABLE 2

Quantities of Benzene Remaining on the Rh Surface after Hydrogenation at 25, 65, and 115°C

% dopant	Quantity of benzene remaining adsorbed (μmol/g catalyst)				R_B
	Without prior hydrogenation	After hydrogenation at 25°C	65°C	115°C	
0	2.2	1.2	1.0	1.0	0.46
0.11	3.5	2.1	1.7	1.4	0.40
0.22	2.6	1.4	0.9	0.5	0.19
0.45	3.8	3.3	2.3	1.0	0.26
0.67	4.4	3.2	2.1	1.2	0.27

TABLE 3

Quantities of Toluene Remaining on the Rh Surface after Hydrogenation at 25 and 115°C

% dopant	Quantity of toluene remaining adsorbed (μmol/g catalyst)			R_T
	Without prior hydrogenation	After hydrogenation at 25°C	115°C	
0	1.7	1.1	1.0	0.59
0.11	3.1	2.0	0.8	0.26
0.22	1.8	1.5	0.6	0.33
0.45	4.0	4.0	1.0	0.25
0.67	2.3	1.6	1.0	0.43

hydrogenated at 25 or 115°C. The results are summarized in Table 3. As in the case of benzene, the R_T values of the W^{6+}-doped catalysts are lower than those of the undoped catalyst, indicating that the hydrogenation reactivity of toluene adsorbed on Rh is enhanced when Rh is dispersed on higher-valence doped TiO_2 carriers. It is also observed that the R_T values are higher than the R_B values, indicating that the hydrogenation reactivity of adsorbed benzene is higher than that of adsorbed toluene.

(b-4) TPSR of adsorbed benzene and toluene. The influence of higher-valence carrier doping on the reactivity of benzene and toluene adsorbed on Rh, was further investigated by a TPSR technique. The aromatic molecules were adsorbed at room temperature and, after purging with He, the gas flow was switched to H_2. Temperature was maintained at this level until production of cyclohexane or methylcyclohexane ceased. The sample was subsequently heated with a heating rate of 23°C/min under H_2 flow. The surface reactions which take place during this procedure are the following. (a) All the weakly adsorbed benzene and part of the weakly adsorbed toluene on the carrier surface are hydrogenated at room temperature. (b) As temperature increases, a portion of the aromatic molecules strongly adsorbed on Rh surfaces are hydrogenated to cyclohexane or methylcyclohexane while another small portion might be desorbed. (c) At high enough temperatures the remaining aromatic molecules decompose on the surface into fractions of the form C_xH_y (32), which, at even higher temperatures, are hydrogenated to CH_4. Thus, the CH_4 profiles can be utilized to assess the strength of benzene or toluene adsorption bonds with the Rh surface.

In the case of benzene, the only species which was detected to desorb in measurable quantities after initiation of temperature programming was CH_4. The CH_4 profiles

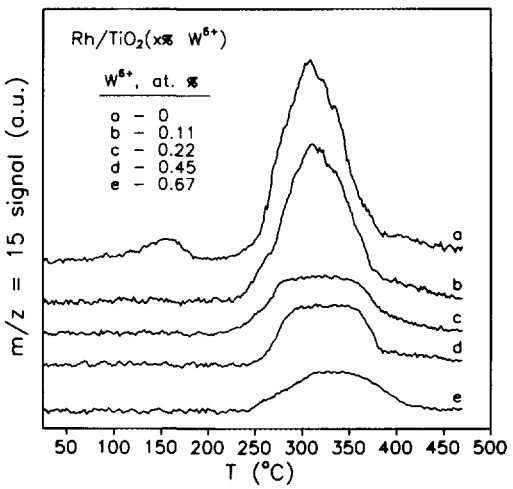

FIG. 8. TPSR profiles of CH_4 produced after benzene adsorption at 25°C on 0.5% $Rh/TiO_2(x\%\ W^{6+})$ catalysts using hydrogen as the carrier gas.

obtained over the $Rh/TiO_2(x\%\ W^{6+})$ catalysts are shown in Fig. 8. In the case of toluene, in addition to CH_4, methylcyclohexane was also observed to desorb at temperatures between 30 and 100°C. This is in agreement with results discussed earlier (26) showing that the hydrogenation reactivity of toluene adsorbed on the surface of the carrier is smaller than that of benzene. The CH_4 profiles obtained during TPSR of adsorbed toluene are shown in Figure 9. From Figs. 8 and 9 it is apparent that, in all cases, CH_4 appears in the temperature range of 250–350°C. Although peak temperatures do not seem to be significantly affected by carrier doping, the quantity

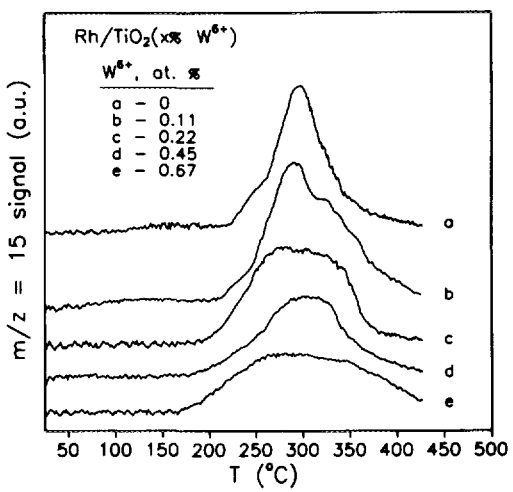

FIG. 9. TPSR profiles of CH_4 produced after toluene adsorption at 25°C on 0.5% $Rh/TiO_2(x\%\ W^{6+})$ catalysts using hydrogen as the carrier gas.

TABLE 4

Relative Quantities of CH_4 Produced during TPSR of Benzene and Toluene over $Rh/TiO_2(x\%\ W^{6+})$ Catalysts

	CH_4 produced from	
% dopant	Benzene	Toluene
0	100	100
0.11	81	64
0.22	47	95
0.45	52	31
0.67	19	59

of CH_4 produced is significantly reduced with increasing dopant concentration, although, as shown in Tables 2 and 3, the quantity of benzene and toluene adsorbed on Rh is higher in the doped catalysts. The fact that no other products were detected implies that the missing benzene or toluene desorbed or reacted in the presence of H_2 at lower temperatures (Figs. 4a and 4b). The relative quantities of CH_4 produced are shown in Table 4, in which the quantity of CH_4 produced over the undoped catalyst has been assigned arbitrarily the value of 100. The reduced quantity of CH_4 produced over the doped catalysts indicates that a smaller portion of benzene or toluene is adsorbed on these catalysts strongly enough so as to remain adsorbed at high temperatures and eventually decompose to CH_4. This result is in good agreement with the TPD results discussed earlier. Furthermore, the position of the CH_4 peak does not seem to be dependent on the aromatic molecule adsorbed, indicating that CH_4 production proceeds through the same intermediates in both cases.

DISCUSSION

The competitive benzene-toluene hydrogenation has often been used as a probe reaction to detect alterations in the electronic structure of metallic surfaces or even to detect alloy formation (19–22). The critical parameter is the ratio of the adsorption coefficients of toluene and benzene, $K_{T/B}$. The methodology is based on the concept that both molecules are bonded to the metal surface via π-bonds, which involve electron transfer from the aromatic ring to the unoccupied d-orbitals of the metal atoms and backdonation from the metal to the π^*-hydrocarbon orbitals (36). It is further assumed that benzene and toluene molecules adsorb nondissociatively and with the same mode, competing for the same sites. The validity of this assumption is supported by EELS (25) and NEXAFS (41) studies, which show that this is indeed the case, at least

for Pt. Since toluene is more of an electron donor that benzene, it forms stronger chemisorption bonds with metallic surfaces (24, 25). This is reflected in the fact that $K_{T/B}$ is always larger than unity. Thus, the larger the electron acceptance capacity of the surface, the larger the value of $K_{T/B}$. This premise is believed to hold within the same metal, if its environment is changed in such a way so as to alter the electronic configuration (e.g. the density of states in the *d*-band or the work function) of the metal crystallites, or even among different metals within the same group (22).

The results presented in Fig. 3 show that the $K_{T/B}$ values observed over Rh supported on higher valence doped TiO_2 carriers decrease significantly upon doping and that the reduction is a function of the concentration of the dopant cation in the matrix of the support. These results imply that the electron acceptor capacity of the metallic surface is reduced as a result of carrier doping. The alteration of the electronic structure of the metallic surface is in the direction of enhanced *d*-electron population and/or decreased surface work function. If these premises are correct, then the benzene and toluene adsorption bonds with the metallic surfaces would be expected to be weakened upon higher valence doping of the TiO_2 carrier. Indeed, this conclusion has been obtained from the TPD and TPSR results of benzene and toluene adsorption on $Rh/TiO_2(x\%\ W^{6+})$ catalysts, as discussed earlier. The weakening of the Rh-benzene or Rh-toluene adsorption bond can be considered as a consequence of the increased electron density of Rh, which makes less favorable the charge transfer from the aromatic molecule to Rh. Similar effects have been observed in the case of benzene adsorption in the presence of electropositive impurities. For example, the heat of adsorption of benzene on a Pt surface that contains K, which decreases the surface work function, is reduced compared to that of the clean Pt surface (42).

The activity of Rh was found to be significantly affected upon doping of the carrier with cations of higher valence, and to be a function of dopant concentration. Both benzene and toluene hydrogenation activity under steady-state reaction conditions were found to increase with increasing dopant concentration in the matrix of the carrier. The TPD and TPSR experiments also revealed enhanced reactivity of benzene and toluene adsorbed on Rh supported upon W^{6+}-doped TiO_2 carriers. The observed enhancement of reactivity under both steady-state and transient conditions is probably due to two factors: these are the weakening of the benzene and toluene adsorption bonds and the increased capacity of the catalysts to adsorb hydrogen which has been observed and reported previously (13, 14).

Alterations in chemisorptive and kinetic parameters of Group VIII metals supported on TiO_2 doped with altervalent cations have been explained in terms of electronic alterations of the metal crystallite surfaces. The alteration of the electron structure of metal surfaces or, more precisely, the alteration of the work function of surface metal atoms, upon doping of a semiconductive carrier with cations of different valence has been explained evoking the boundary layer theory of metal–semiconductor contacts (13). According to this theory, when a metal is in contact with a semiconductor, the Fermi level of the two solids must be at equal height at thermodynamic equilibrium (43–45). This is achieved by charge transfer between the metal and the semiconductor. When the Fermi level of the semiconductor is higher than that of the metal, as in the case of Group VIII metals and higher valence doped TiO_2 (13), electrons are transferred from the semiconductor to the metal and penetrate a small distance (Thomas–Fermi screening distance) into the metal. Thus, a dipole is formed at the metal-carrier interfacial area, the interface metal atoms being negatively charged, while the semiconductor depletion region is positively charged.

The hypothesis that charge is being transferred from the higher-valence doped semiconducting carrier into the metal crystallites is well-established [Ref. (43) and references therein]. The question which still remains unanswered is whether the amount of charge transferred is sufficient to alter not only the electronic properties of the interface metal atoms, but also those of the surface metal atoms. Alternatively, the question is whether the interaction at the metal–semiconductor interface produces a localized or a long-range effect. The localized or short-range effect refers to the metal atoms in contact with the carrier, which are also exposed to the gas phase, thus participating in chemisorption and reaction phenomena. These atoms are under the influence of strong electrostatic fields, due to the existence of the dipole at the interface, which could alter their adsorptive properties. In small metal particles the number of atoms at the three-phase boundary (metal–semiconductor–gas) can be a significant fraction of the total number of atoms in the crystallite. The long-range effect refers to changes in the *d*-density, as well as, alteration of the work function of surface metal atoms induced by lowering of the chemical potential of the metal crystallites, as a result of their contact with the semiconductor. Since the chemical potential is a bulk property of the metal particles and since the surface potential of the free metallic surface is not altered, any changes in the chemical potential should reflect equal changes in the work function of the metal crystallites. Measurable alterations in the chemical potential can be induced only when the metal particles are sufficiently small. It must also be pointed out that small alterations in the work function of metal atoms can significantly influence the chemisorptive and subsequently kinetic behavior of the metal atoms.

CONCLUSIONS

The results obtained in the present study provide further indications that a metal-support interaction of the electronic type is taking effect when Rh is dispersed on W^{6+}-doped TiO_2. The observations that the ratio $K_{T/B}$ of the adsorption constants of toluene and benzene decreases and that the adsorption bonds of benzene and toluene with the Rh surface weaken on doped catalysts, suggest that in this case the Rh surface is of increased electron density and/or lower work function. This has been attributed to electron transfer from the doped supports to the Rh crystallite, as predicted from the metal-semiconductor contact theory.

REFERENCES

1. Sadeghi, H. R., and Henrich, V. E., *J. Catal.* **87,** 279 (1984).
2. Simeons, A. J., Baker, R. T. K., Droyer, D. J., and Madon, R. J., *J. Catal.* **86,** 359 (1984).
3. Ko, C. S., and Gorte, R. J., *J. Catal.* **90,** 59 (1984).
4. Hermann, J.-M., *J. Catal.* **118,** 43 (1989).
5. Resasco, D. E., and Haller, G. L., *J. Catal.* **82,** 279 (1983).
6. Schwab, G. M., *Adv. Catal.* **27,** 1 (1987).
7. Solymosi, F., *Catal. Rev.* **1,** 233 (1967).
8. Akubuiro, E. C., and Verykios, X. E., *J. Catal.* **103,** 320 (1987).
9. Akubuiro, E. C., and Verykios, X. E., *J. Catal.* **113,** 106 (1988).
10. Akubuiro, E. C., and Verykios, X. E., *J. Phys. Chem. Solids* **50,** 17 (1989).
11. Akubuiro, E. C., Ioannides, T., and Verykios, X. E., *J. Catal.* **116,** 590 (1989).
12. Akubuiro, E. C., Verykios, X. E., and Ioannides, T., *Appl. Catal.* **46,** 297 (1989).
13. Ioannides, T., and Verykios, X. E., *J. Catal.* **145,** 479 (1994).
14. Ioannides, T., Verykios, X. E., Tsapatsis, M., and Economou, C., *J. Catal.* **145,** 491 (1994).
15. Zhang, Z., Kladi, A., and Verykios, X. E., *J. Catal.* **148,** 737 (1994).
16. Solymosi, F., Tombacz, I., and Koszta, J., *J. Catal.* **95,** 578 (1985).
17. Yoshitake, H., and Iwasawa, Y., *J. Phys. Chem.* **96,** 1329 (1992).
18. Vayenas, C. G., Bebelis, S., Yentekakis, I. V., and Lintz, H. G., *Catal. Today* **11,** 303 (1992).
19. Frank, J.-P., and Gil, J. M., *Comptes Rendu* Serie C **287,** 85 (1978).
20. Tri, T. M., Massardier, J., Gallezot, P., and Imelik, B., in "Studies in Surface Science and Catalysis," Vol. 11, Metal-Support and Metal Additive Effects in Catalysis, p. 141, Elsevier, Amsterdam, 1982.
21. Szymanski, R., Charcosset, H., Gallezot, P., Massardier, J., and Tournayan, L., *J. Catal.* **97,** 366 (1986).
22. Phuong, T. T., Massardier, I., and Gallezot, P., *J. Catal.* **102,** 452 (1986).
23. Ioannides, T., and Verykios, X. E., *J. Catal.* **140,** 353 (1993).
24. Minot, C., and Gallezot, P., *J. Catal.* **123,** 341 (1990).
25. Abon, M., Bertolini, J. C., Billy, J., Massardier, J., and Tardy, B., *Surf. Sci.* **162,** 395 (1985).
26. Ioannides, T., and Verykios, X. E., *J. Catal.* **143,** 175 (1993).
27. Suda, Y., *Langmuir* **4,** 147 (1988).
28. Nagao, M., and Suda, Y., *Langmuir* **5,** 42 (1989).
29. Low, M. J. D., McNelis, E., and Mark, H., *J. Catal.* **100,** 328 (1986).
30. Primet, M., Garbowski, E., Mathieu, M. V., and Imelik, B., *J. Chem. Soc. Faraday Trans. I* **76,** 1942 (1980).
31. Koel, B. E., Crowell, J. E., Bent, B. E., Mate, C. M., and Somorjai, G. A., *J. Phys. Chem.* **90,** 2949 (1986).
32. Koel, B. E., Crowell, J. E., Mate, C. M., and Somorjai, G. A., *J. Phys. Chem.* **88,** 1988 (1984).
33. Palazov, A., Bonev, C., Shopov, D., Lietz, G., Sárkány, A., and Völter, J., *J. Catal.* **103,** 249 (1987).
34. Candy, J. P., Fouilloux, P., and Imelik, B., *Nouv. J. Chim.* **2,** 45 (1978).
35. Martin, G. A., and Dalmon, J. A., *J. Catal.* **75,** 233 (1982).
36. Garfunkel, E. L., Minot, C., Gavezzotti, A., and Simonetta, M., *Surf. Sci.* **167,** 177 (1986).
37. Tsai, M. C., and Muetterties, E. L., *J. Phys. Chem.* **86,** 5067 (1982).
38. Friend, C. M., and Muetterties, E. L., *J. Am. Chem. Soc.* **103,** 773 (1981).
39. Orozco, J. M., and Webb, B., *Appl. Catal.* **6,** 67 (1983).
40. Jacob, P., and Menzel, D., *Surf. Sci.* **201,** 503 (1988).
41. Johnson, A. L., Muetterties, E. L., and Stöhr, J., *J. Amer. Chem. Soc.* **105,** 7183 (1983).
42. Garfunkel, E., Maj, J. J., Frost, J. C., Farlas, M. H., and Somorjai, G. A., *J. Phys. Chem.* **87,** 3629 (1989).
43. Tyagi, M. S., in "Metal-Semiconductor Schottky Barrier Junctions and Their Applications" (B. L. Sharma, Ed.) Plenum, New York, 1984.
44. Sze, S. M., "Physics of Semiconductor Devices," 2nd ed., Wiley, New York, 1981.
45. Brillson, L. J., *Surf. Sci. Rep.* **2,** 123 (1982).